Receptor tyrosine kinase Met promotes cell survival via kinase-independent maintenance of integrin α3β1

Lia Tesfay[†], Veronique V. Schulz[†], Sander B. Frank, Laura E. Lamb, and Cindy K. Miranti*
Laboratory of Integrin Signaling and Tumorigenesis, Van Andel Research Institute, Grand Rapids, MI 49503

ABSTRACT Matrix adhesion via integrins is required for cell survival. Adhesion of epithelial cells to laminin via integrin α3β1 was previously shown to activate at least two independent survival pathways. First, integrin α3β1 is required for autophagy-induced cell survival after growth factor deprivation. Second, integrin α3β1 independently activates two receptor tyrosine kinases, EGFR and Met, in the absence of ligands. EGFR signaling to Erk promotes survival independently of autophagy. To determine how Met promotes cell survival, we inhibited Met kinase activity or blocked its expression with RNA interference. Loss of Met expression, but not inhibition of Met kinase activity, induced apoptosis by reducing integrin α3β1 levels, activating anoikis, and blocking autophagy. Met was specifically required for the assembly of autophagosomes downstream of LC3II processing. Reexpression of wild-type Met, kinase-dead Met, or integrin α3 was sufficient to rescue death upon removal of endogenous Met. Integrin α3β1 coprecipitated and colocalized with Met in cells. The extracellular and transmembrane domain of Met was required to fully rescue cell death and restore integrin α3 expression. Thus Met promotes survival of laminin-adherent cells by maintaining integrin α3β1 via a kinase-independent mechanism.

INTRODUCTION

Adhesion of cells to the extracellular matrix via integrins is required for cell survival. Death induced by loss of cell adhesion, called anoikis, is mediated through both intrinsic and extrinsic apoptotic pathways (Frisch and Screaton, 2001; Marconi *et al.*, 2004; Valentijn *et al.*, 2004; Gilmore, 2005). Detachment induces extrinsic apoptosis through FADD-dependent activation of caspase 8 and FOXO1/3a suppression of the caspase 8 antagonist c-Flip, which may or may not involve Fas/FasL interactions (Frisch, 1999; Rytomaa *et al.*, 1999; Aoudjit and Vuori, 2001; Rosen *et al.*, 2002; Skurk *et al.*, 2004; Gan *et al.*, 2009). Conversely, adhesion lowers Fas expression while at the same time inducing c-Flip by up-regulating Erk signaling (Aoudjit and Vuori, 2001). Integrin signaling also up-regulates antiapoptotic proteins such as Bcl-2, Bcl-xL, and Mcl-1 via Akt, Jnk, Erk, or Src and simultaneously prevents anoikis-dependent activation of the proapoptotic proteins Bid, Bmf, Bim, and Bak/Bax (Frisch *et al.*, 1996; Flusberg *et al.*, 2001; Puthalakath *et al.*, 2001; Coll *et al.*, 2002; Reginato *et al.*, 2003; Harnois *et al.*, 2004; Valentijn and Gilmore, 2004; Schmelzle *et al.*, 2007; Boisvert-Adamo and Aplin, 2008; Boisvert-Adamo *et al.*, 2009; Owens *et al.*, 2009).

Another mechanism by which integrins promote survival is through activation of the receptor tyrosine kinase (RTK) epidermal growth factor receptor (EGFR). Adhesion of epithelial cells to laminin is sufficient to activate EGFR in the absence of ligand (Bill *et al.*, 2004). EGFR activation by adhesion to laminin via integrin α3β1 leads to Erk signaling, which is required for survival (Manohar *et al.*, 2004; Edick *et al.*, 2007). Under starvation conditions, integrin α3β1 in epithelial cells is also required to robustly activate autophagy-dependent survival (Edick *et al.*, 2007). However, the mechanism by which autophagy is controlled by integrin α3β1 remains to be determined.

FIGURE 1: Loss of Met induces cell death. PrECs transfected with Met siRNAs (siMet1251, siMet4268) or controls (siScr, lipid) or infected with adenoviruses containing Met shRNA (shMet) or control viruses (shMetMut, shScr, vector, mock) at an MOI of 2 in starvation medium, plated on endogenous laminin matrix, and analyzed 72 h later. (A) Total Met in cell lysates measured by immunoblotting; tubulin is the loading control. (B) Cells expressing the indicated RNAi visualized under phase-contrast microscopy. (C) Cell viability measured by trypan blue exclusion before (0 h) or 72 h after siRNA transfection. (D) Cellular ATP measured 72 h after siRNA transfection or 24 h after 1 μM staurosporine (Str) treatment. Error bars are SD; $n = 3$; p values are as indicated.

RESULTS

Primary prostate epithelial cells (PrECs) isolated from patients and cultured in defined medium secrete an endogenous laminin matrix to which the cells adhere via integrins α3β1 and α6β4 (Gmyrek et al., 2001; Edick et al., 2007). Our previous studies demonstrated that survival of PrECs on this matrix in the absence of growth factors is dependent on integrin α3β1 (Edick et al., 2007). For all the assays reported here, the cells are first genetically manipulated and then allowed to adhere to their endogenous matrix in the absence of growth factors.

PrECs were transfected with control or Met-specific siRNAs or infected with Met-specific adenoviral short hairpin RNAs (shRNAs). After adhesion, Met protein expression was monitored by immunoblotting. Met expression was reduced 80–90% by Met-specific RNA interference (RNAi; Figure 1A) but not by scrambled or mutant RNAi or lipid-only, mock-infected, or vector controls. There was a corresponding decrease in the number of cells in Met RNAi–treated cells and cells displayed a rounded morphology (Figure 1B). This was accompanied by a ninefold reduction in cell viability (Figure 1C) and a twofold decrease in intracellular ATP (Figure 1D). Thus Met is required for normal cell survival.

Inhibition of Met expression by RNAi reduced both full-length caspase 3 and Bcl-xL expression and increased cleaved caspase3 (Figure 2, A and B). In addition, >70% of the cells stained positive for annexin V (Figure 2C), and there was an approximately fourfold increase in caspase 3/7 activity, equivalent to that seen with the general apoptosis inducer staurosporine (Figure 2, D and E). Thus Met promotes survival by preventing apoptosis.

Treatment of starved cells with either of two different Met-specific inhibitors, SU11274 or PHA665752 (Christensen et al., 2003; Humbert et al., 2013), reduced Met activity (Figure 3A) but had no effect on cell morphology or cell number (Figure 3B), did not alter intracellular ATP levels (Figure 3C), and did not increase caspase 3/7 activity (Figure 3D). Several different drug concentrations produced no effects on cell viability, even after the cells were treated for 5 d with repeated drug replenishment. Thus loss of Met protein specifically, rather than its kinase activity, induces apoptosis.

To further validate the dependence of normal epithelial cells on Met for survival, we used adenoviral green fluorescent protein (GFP)–Cre to knock out Met expression in prostate epithelial cells isolated from Met floxed mice (Figure 3E). Cells having the highest concentration of GFP-Cre virus, as imaged by fluorescence, detached from the plate, leaving a zone of clearing. Infection of cultures with GFP-only virus resulted in no rounding, no detachment, and no loss of cells, even in areas with high GFP expression. Epithelial cells were also isolated from Met floxed mice crossed to Cre-ER^TM mice, and the cells were treated with tamoxifen to induce Met loss. Tamoxifen treatment reduced the number of adherent

The RTK Met is expressed in epithelial and endothelial cells and promotes cell proliferation, migration, and morphogenesis (Knudsen and Vande Woude, 2008). Like EGFR, integrins activate Met in the absence of ligand (Wang et al., 1996; Sridhar and Miranti, 2006), and ligand-independent activation of Met promotes tumorigenesis and invasion (Wang et al., 2001; Sridhar and Miranti, 2006). Furthermore, blocking Met expression by small interfering RNA (siRNA) induces cell death in metastatic tumor cell lines, indicating that Met is also important for tumor cell survival (Shinomiya et al., 2004). Studies in Met conditional knockout mice suggest that Met regulates normal cell survival as well. Liver hepatocytes from albumin-Cre Met^−/− mice are much more sensitive to FasL-induced cell death and contain elevated levels of reactive oxygen species (Huh et al., 2004; Gomez-Quiroz et al., 2008). One possible mechanism for increased Fas sensitivity in Met-null cells could involve enhanced Fas dimerization due to disruption of Met/Fas complexes (Wang et al., 2002; Zou et al., 2007). Because Fas/FasL signaling is suppressed by integrins, we tested the hypothesis that Met activation via laminin integrins regulates normal cell survival.

FIGURE 2: Loss of Met induces intrinsic apoptosis. Met expression suppressed in PrECs with RNAi and analyzed 72 h after adhesion to endogenous laminin. Error bars are SD; $n = 4$. (A) Met, full-length caspase 3, Bcl-xL, and tubulin measured by immunoblotting. (B) Met, cleaved caspase3, and glyceraldehyde-3-phosphate dehydrogenase (GAPDH) measured by immunoblotting. (C) Annexin V positivity measured by immunostaining. (D, E) Caspase 3/7 activity measured after (D) transfection or (E) infection with indicated RNAi or treatment with 1 μM staurosporine (Str). mshMet is a mutant shRNA that does not target Met.

cells compared with vehicle-treated controls (Figure 3G). The loss of Met protein was verified by immunoblotting, and there was a corresponding decrease in full-length caspase 3 and Bcl-xL levels in the cultures (Figure 3, F and H). Thus loss of Met in both human and mouse primary epithelial cell cultures resulted in cell death.

To further test Met kinase dependence, we infected cells with viruses expressing an empty vector, wild-type (WT) Met (full-length, siMet-resistant), or a kinase-inactive (DN) Met mutant. Endogenous Met was then removed by siRNA. Exogenous Met in the siRNA-treated cells was expressed at levels equivalent to endogenous Met in the control cells (Figure 4A). The Met mutant was not active, as measured by a lack of tyrosine phosphorylation at the activation site. Furthermore, activation of endogenous Met was also suppressed (Figure 4B). Expression of either wild-type or kinase-inactive Met was sufficient to prevent cell morphology changes (Figure 4C), cell death (Figure 4D), caspase 3/7 activation (Figure 4E), and loss of Bcl-xL (Figure 4A) induced by siMet. Thus the kinase activity of Met is not required for cell survival.

Cell survival on laminin is mediated through integrin α3β1–dependent activation of the EGFR/Erk signaling pathway (Manohar et al., 2004; Edick et al., 2007). Met siRNA decreased EGFR and Erk activity (Figure 5A). The loss of EGFR/Erk signaling could be due to nonspecific effects of intrinsic caspase activation mediated by Met loss rather than a direct effect of Met loss. However, zVAD at concentrations sufficient to block caspase 3/7 activation (Figure 5B) did not block the decrease in EGFR (unpublished data) or Erk activation induced by siMet (Figure 5C), indicating that cell death is occurring downstream of EGFR/Erk inhibition. Thus loss of Met prevents cell survival mediated by integrin α3β1–dependent EGFR/Erk signaling.

We also previously showed that integrin α3β1–mediated adhesion promotes the survival of growth factor–starved cells by induc-

ing autophagy (Edick et al., 2007). The level of autophagy, as measured by immunoblotting for LC3-II, was much higher in siMet-treated cells than in cells maintained in full growth medium or treated with scrambled siRNA (Figure 5D), suggesting that loss of Met leads to enhanced autophagy. However, inhibiting autophagic flux through the lysosome with chloroquine in siMet-treated cells resulted in a similar accumulation of LC3-II as without chloroquine and to a much greater degree than was seen with the scrambled control. These data indicate that although LC3-II is accumulating, it is not being degraded. Degradation of LC3-II depends on autophagosome fusion with lysosomes. The lysosomal marker LAMP2 is increased during autophagosome/lysosome fusion (Saftig et al., 2008). Accordingly, LAMP2 levels were increased in growth factor–deprived, scrambled siRNA–treated cells relative to cells maintained in complete growth medium (Figure 5D). However, LAMP2 levels were not elevated after Met loss, even after the lysosome was blocked with chloroquine (Figure 5D), consistent with a reduction in autophagy-induced lysosomal function.

Furthermore, when autophagy was measured by quantifying the accumulation of GFP-LC3 puncta, we found a 2.5-fold reduction in puncta in siMet-treated cells (Figure 5, E and F), further demonstrating that although LC3-II is accumulating, it is not effectively assembled into autophagosomes. The increase in LC3-II levels in siMet-treated cells was not due to an indirect effect of caspase activation, as treatment with zVAD did not reverse LC3-II accumulation (Figure 5G). The excessive accumulation of LC3-II was reversed when WT or kinase-inactive Met was exogenously expressed in siMet-treated cells (Figure 5H). Thus Met, independently of its kinase activity, is required to assemble autophagosomes in growth factor–starved cells.

Two of the survival pathways we previously described to be controlled by integrin α3β1—EGFR/Erk signaling and autophagy (Edick et al., 2007)—are disrupted in cells lacking Met. This suggests that
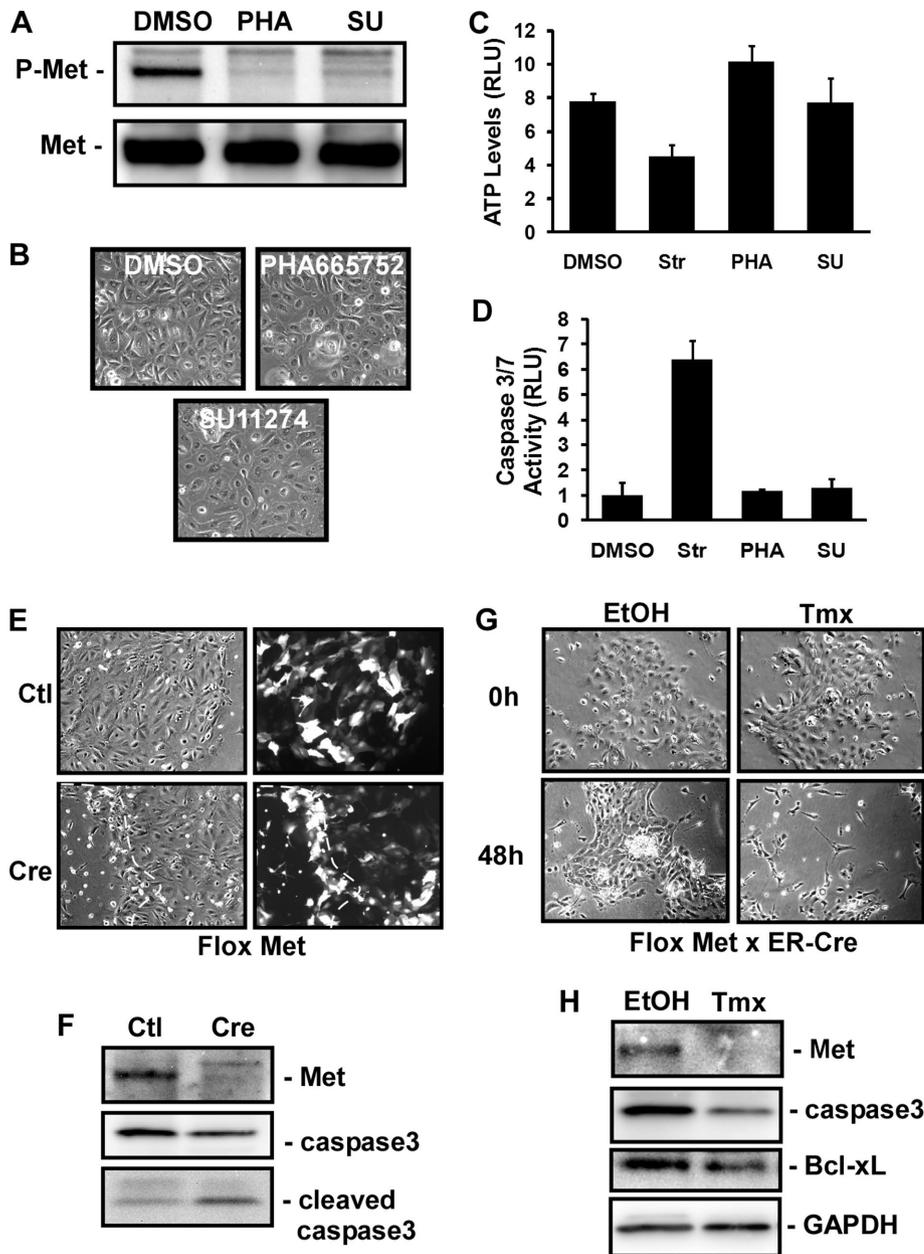
FIGURE 3: Loss of Met, but not its kinase activity, induces cell death. (A–D) Laminin-adherent PrECs treated with vehicle (DMSO), 0.2 μM PHA665752 (PHA), or 20 μM SU11274 (SU) for 72 h in starvation medium. (A) Met activity and total Met measured by immunoblotting of Met immunoprecipitates with anti-phosphotyrosine (P-Met) and Met antibodies. (B) Drug-treated cells imaged under phase-contrast light microscopy. (C) ATP levels and (D) caspase 3/7 activity measured in drug-treated cells compared with cells treated with 1 μM staurosporine (Str). Error bars are SD; $n = 3$. (E, F) Prostate epithelial cells isolated from Met$^{fl/fl}$ mice and Met loss induced by infection with virus expressing GFP (Ctl) or GFP-Cre (Cre). (E) Cells imaged under phase-contrast (left) or epifluorescence (right) microscopy 24 h after Cre infection. White dashed line marks the boundary between live and dead cells. (F) Met and full-length or cleaved caspase 3 measured by immunoblotting. (G, H) Prostate epithelial cells isolated from Met$^{fl/fl}$ mice crossed to Cre-ER^{TM} mice and Met knockout induced by treatment with vehicle (EtOH) or 1.5 μM tamoxifen (Tmx). (G) Cells imaged under phase-contrast light microscopy before treatment (0 h) or 48 h later. (H) Met, full-length caspase 3, Bcl-xL, and GAPDH measured by immunoblotting.

that cell death per se is not inducing α3 loss. A decrease in total integrin α3 and α6, as detected by immunoblotting, was seen much later, 72 h after siMet treatment (Figure 6B). However, this late decrease in α6, unlike that in α3, was reversed by inhibition of caspase 3/7. This is consistent with reports demonstrating a caspase 3/7 cleavage site in integrin β4, a partner of α6 (Chmielowiec et al., 2007). Thus loss of α3β1 is upstream, whereas loss α6β4 is downstream, of caspase activation. Loss of integrin α3 was accompanied by a reduction in integrin β1, its associated subunit partner (Figure 6C); this partial loss is likely due to β1 pairing with other remaining α subunits. Thus the differential effects on integrin α6β4 versus integrin α3β1 highlight the specificity of Met in targeting integrin α3β1.

Exogenous expression of WT or DN Met in siMet-treated cells restored Erk signaling and integrin α3 expression (Figure 6D). Furthermore, restoring integrin α3 expression alone in siMet-treated cells (Figure 6E) was sufficient to rescue cell death (Figure 6F). Thus Met mediates cell survival through integrin α3β1. To determine the universality of the Met/α3β1 relationship, we assessed the effect of Met loss on α3β1 expression and signaling in human umbilical vein endothelial cells (HUVECs). HUVECs express Met, EGFR, and integrin α3β1 and adhere to laminin; therefore they may share a similar survival mechanism. Indeed, reductions in integrin α3, Erk activation, and Bcl-xL expression (Figure 6G), as well as induction of cell death (unpublished results), were observed in HUVEC cells transfected with siMet relative to the scrambled siRNA controls. Thus Met mediates survival by maintaining integrin α3 expression in at least two different cell types.

The absence of integrin α3β1 in Met-deficient cells suggests that Met loss triggers anoikis. Inhibition of caspase 8/10 with zIETD or Fas with ZB4 neutralizing antibody, individually or in combination, resulted in a partial rescue of cell viability (Supplemental Figure S1A). Similarly, inhibition of late-stage caspases by zVAD partially rescued cell viability. Simultaneous inhibition of caspase 8/10 and late-stage caspases completely restored cell viability. Treatment with zIETD, Fas blocking antibody, or zVAD (Figure 5) failed to restore integrin α3 or EGFR/Erk signaling (Supplemental Figure S1B). Thus the proximal regulation of α3β1

loss of Met disrupts integrin α3β1. Accordingly, we observed a 2.5-fold decrease in integrin α3 surface expression and a small, reproducible (but not statistically significant) decrease in surface expression of integrin α6 and β4 24 h after siMet treatment (Figure 6A). The decrease in α3 expression was not reversed by zVAD, indicating

by Met prevents subsequent activation of intrinsic and extrinsic cell death pathways; that is, removal of Met causes anoikis by reducing integrin α3β1 expression, leading to Fas activation.

Reciprocal coimmunoprecipitations indicated that a complex can be detected between Met and integrin α3 (Figure 7A) but not
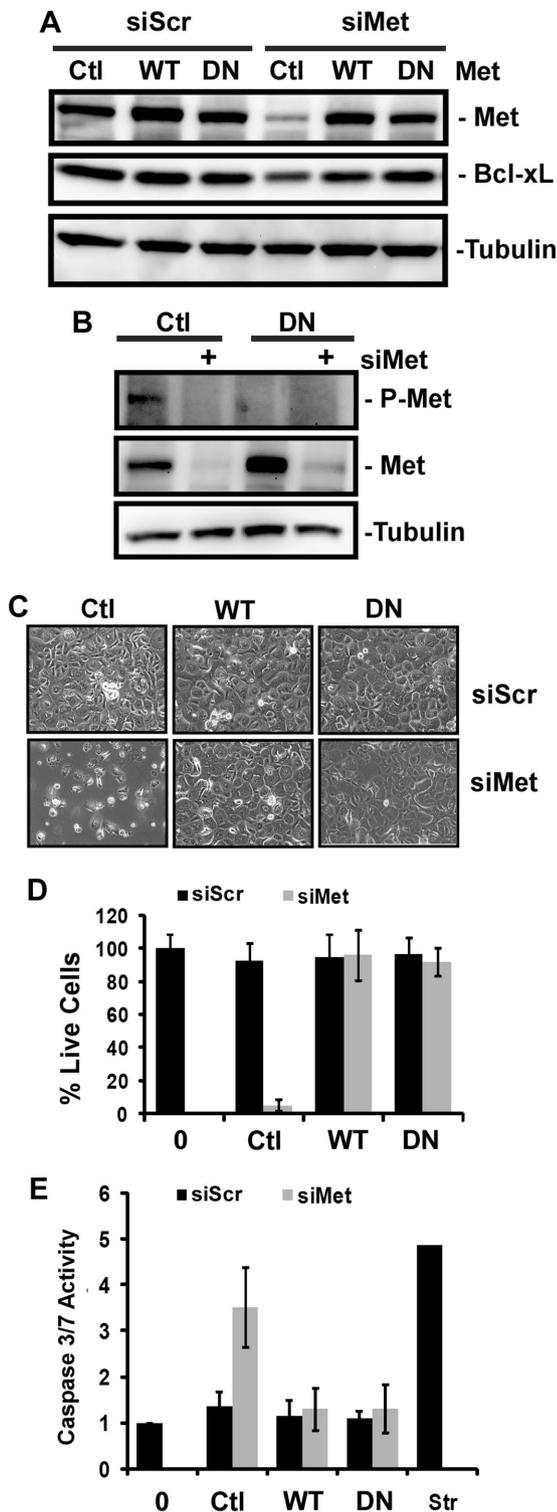
FIGURE 4: Kinase-inactive Met rescues cell survival. PrECs infected with empty adenovirus vector (Ctl) or virus expressing human siRNA-resistant wild-type (WT) or kinase-dead (DN) Met and then 16 h later transfected with Met (siMet) or scrambled (siScr) siRNA in starvation medium. Error bars are SD; $n = 4$. (A) Immunoblots of Met, Bcl-xL, and tubulin after adhesion to endogenous laminin for 48 h. (B) Immunoblots of activated (P-Met [Y1234/35]) and total Met (Met) and tubulin from cells expressing endogenous (Ctl) or DN Met. (C) Cells imaged under phase-contrast light microscopy. (D) Cell viability assayed by trypan blue exclusion. (E) Caspase 3/7 activity compared with cells treated with 1 μM staurosporine (Str).

between Met and integrin α6; this is in keeping with our previous findings that loss of α6 does not induce significant cell death (Edick et al., 2007) and loss of integrin α6 is not directly regulated by Met (Figure 6B). Immunofluorescence staining and confocal microscopy further showed colocalization of Met and integrin α3 at the basal surface of cell–cell junctions (Figure 7B). We blocked proteasome-mediated degradation with MG132 or lactacystin or lysosomal degradation with chloroquine. Inhibition of the lysosomal pathway, but not the proteasome, prevented the loss of both Met and integrin α3 protein upon Met mRNA knockdown (Figure 7C). Together these data indicate that Met and integrin α3 coexist in a complex at the cell membrane and both are targeted for degradation via the lysosome when new Met protein expression is inhibited by siRNA.

We next determined which domain on Met is required for cell survival and to maintain integrin α3 expression. First we tested whether the truncated, intracellular, constitutively active Met mutant Tpr-Met (Pomerleau et al., 2014) could rescue cell survival and integrin α3 expression. Tpr-Met is not targeted by our siRNA, and its expression in siMet-treated cells completely rescued cell death (Supplemental Figure S2A), but it failed to rescue integrin α3β1 expression (Supplemental Figure S2B). Constitutively active Tpr-Met can activate Erk (Pomerleau et al., 2014), and since Erk is required for PrEC survival (Edick et al., 2007), we assessed Erk activation in the Tpr-Met–expressing cells. Tpr-Met was sufficient to rescue Erk activity, induce Bcl-xL, and prevent caspase 3 cleavage (Supplemental Figure S2C). Thus Tpr-Met rescued cell death independently of integrin α3β1 by up-regulating Erk signaling.

We next generated an siMet-resistant Met mutant in which most of the cytoplasmic domain was deleted (ΔCT). The cytoplasmic deletion exposes the Y1003 Cbl E3-ligase binding site, which could affect Met and/or integrin α3 turnover. Therefore we also generated a Y1003F ΔCT mutant. Expression of either WT or Y1003F ΔCT Met was sufficient to rescue death induced by siMet (Figure 7D). Integrin α3 expression was also restored by both mutants (Figure 7E). Finally, we exposed siMet-treated cells to recombinant Met extracellular domain protein, which partially rescued death in a dose-dependent manner (Figure 7F). However, this ectodomain was not sufficient to restore integrin α3 expression (unpublished data). Thus both the extracellular and transmembrane domains of Met are required to fully prevent cell death and restore integrin α3 expression.

DISCUSSION

In this study, we identified a new mechanism by which the receptor tyrosine kinase Met promotes cell survival. Specifically, Met is required to maintain adequate levels of integrin α3β1 on the cell surface to prevent activation of cell death pathways and maintain autophagic flux (Figure 8). The ability of Met to support this survival pathway is independent of its kinase activity but requires the extracellular and transmembrane domains. Our previous studies demonstrated that integrin α3β1–mediated adhesion to matrix activates EGFR/Erk signaling to promote survival (Edick et al., 2007). Because loss of Met interferes with integrin α3β1, the EGFR/Erk signaling pathway is also disrupted. Thus we defined three distinct signaling pathways downstream of Met/α3β1 that promote epithelial survival on matrix: EGFR/Erk, Fas, and autophagy.

Our data demonstrate that Met has a function that extends beyond its well-characterized role as a receptor tyrosine kinase. Although this is the first description of a nonkinase function for cytoplasmic-truncated Met, it has been demonstrated that several kinases have functions independent of their catalytic activity. Loss of EGFR by siRNA, but not inhibition of its kinase activity, kills PC3
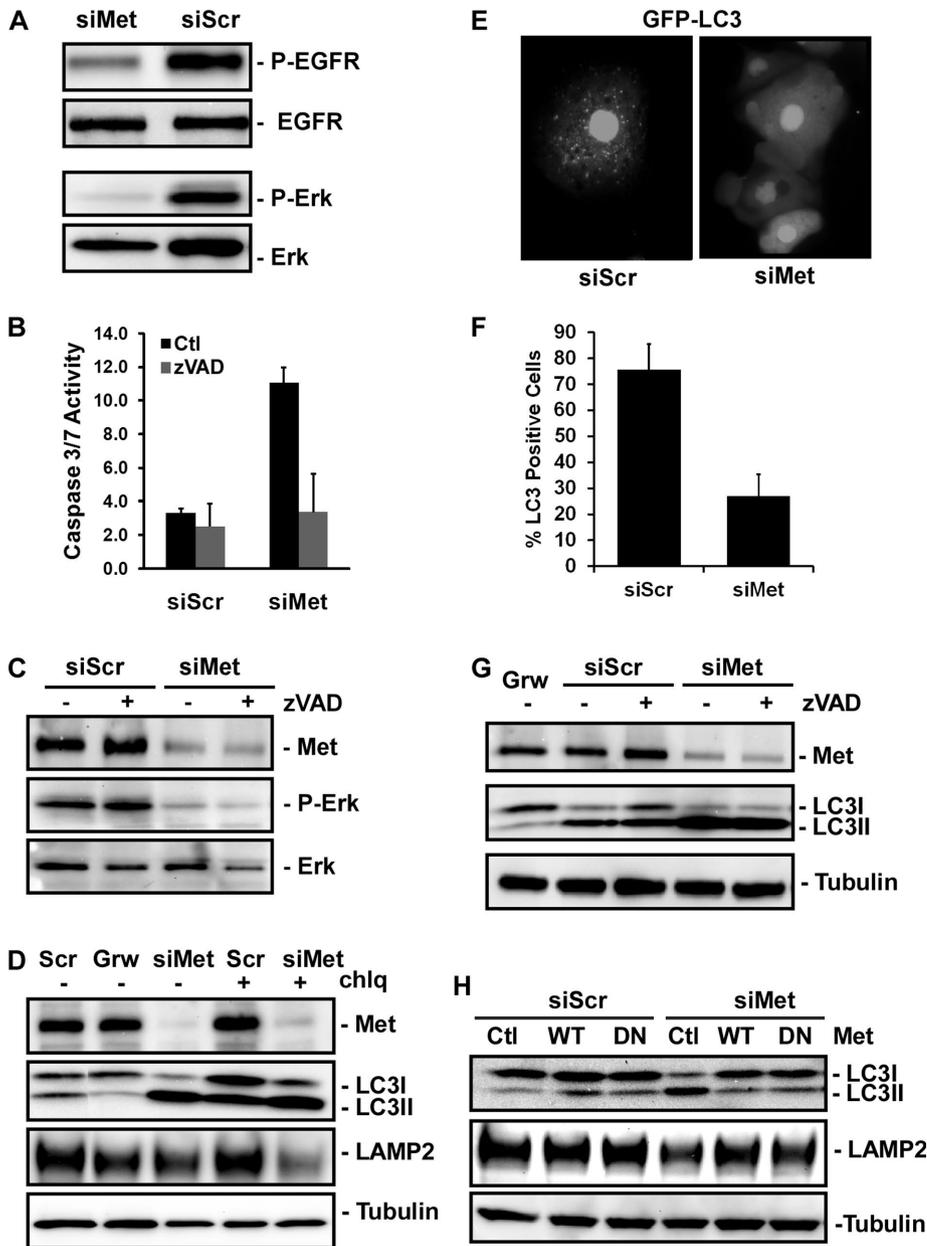
FIGURE 5: Met is required for EGFR/Erk survival signaling and autophagy. PrECs transfected with Met (siMet) or scrambled (siScr) siRNA in starvation medium and assessed 72 h after adhesion to endogenous laminin. Error bars are SD; $n = 3$. (A) EGFR activation (P-EGFR) measured by immunoblotting of EGFR immunoprecipitates using anti-phosphotyrosine antibodies. Erk activation (P-Erk) measured by immunoblotting of cell lysates with anti–phospho-Erk antibodies. (B) Measurement of caspase 3/7 activity with or without zVAD. (C) Met, activated Erk (P-Erk), and total Erk measured by immunoblotting with or without zVAD. (D) Met, LC3I/II, LAMP2, and tubulin in siRNA-transfected cells after treatment with vehicle (–) or 4 μM chloroquine (+ chlq) measured by immunoblotting; Grw, untreated cells maintained in full growth medium. (E, F) PrECs infected with adenovirus expressing GFP-LC3 before siRNA transfection. (E) Laminin-adherent cells were visualized by epifluorescence microscopy 48 h after siRNA transfection. (F) Percentage of cells (within five different fields containing 10 or more puncta per cell) classified as LC3 positive. (G) Met, LC3I/II, LAMP2, and tubulin in siRNA-transfected cells after treatment with vehicle (–) or 20 μM zVAD (+) measured by immunoblotting. (H) PrECs were infected with empty adenovirus vector (Ctl) or virus expressing human siRNA-resistant wild-type (WT) or kinase-dead (DN) Met 16 h before siRNA transfection. Met, LC3I/II, LAMP2, and tubulin were measured by immunoblotting.

et al., 2008; Garcia-Martinez et al., 2010; Luo et al., 2013). In many of these cases, the mechanism involves a scaffolding function that brings several molecules together. These studies further indicate that simply targeting the catalytic activity of a kinase implicated in disease may not be sufficient to fully impede all of its functions.

Defining the exact nature of the Met and integrin α3–interacting complex will require further extensive characterization. The extracellular domain of the integrin α3 subunit is known to bind directly to the tetraspanin CD151 extracellular domain (Yauch et al., 2000; Berditchevski et al., 2001). Several studies suggest there are functional interactions between tetraspanins and Met (Sridhar and Miranti, 2006; Todeschini et al., 2007; Klosek et al., 2009). CD151 overexpression favors cell migration, and CD151 loss in mice prevents wound healing in the skin, as also seen in Met-null keratinocytes (Cowin et al., 2006; Chmielowiec et al., 2007). One study also linked CD151 with epithelial branching in vitro (Klosek et al., 2009), a defect seen in Met- and integrin α3-null kidneys (Kreidberg et al., 1996; Ishibe et al., 2009). Thus tetraspanins could provide a link between Met and integrin α3β1. However, loss of CD151 does not affect the expression of integrin α3β1 (Cowin et al., 2006), indicating that other factors are likely to be involved.

The idea that Met promotes cell survival was nicely demonstrated in conditional Met-null mice. Hepatocytes lacking Met rapidly die from apoptosis after activating Fas receptor (Huh et al., 2004). Met and Fas are known to interact with each other, and Met suppresses Fas by blocking ligand binding via a region on the extracellular domain of Met (Zou et al., 2007). However, our data indicate that loss of Met triggers death by activating Fas through a loss of integrin α3β1. We also find that the extracellular domain of Met is required. Thus the ability of Met to suppress Fas-induced cell death is likely mediated through α3β1.

Although the induction of anoikis is well characterized with respect to the intrinsic and extrinsic apoptosis pathways (Taddei et al., 2012), our study reveals more details about how integrins promote survival through autophagy (Edick et al., 2007). Our data demonstrate that the step in autophagy that is targeted by Met/α3β1 lies between LC3-II processing, which is still intact in Met/α3-negative cells, and the assembly/fusion of autophagosomes with lysosomes,

tumor cells (Weihua et al., 2008). Other examples of molecules with reported kinase-independent functions include FAK, Src, PAK, EphB2, and ILK (Grunwald et al., 2001; Zervas et al., 2001; Higuchi which is impaired. This is seen by the dramatic accumulation of LC3-II but lack of subsequent degradation and the failure to form puncta, that is, to assemble on autophagosomal membranes. Our study
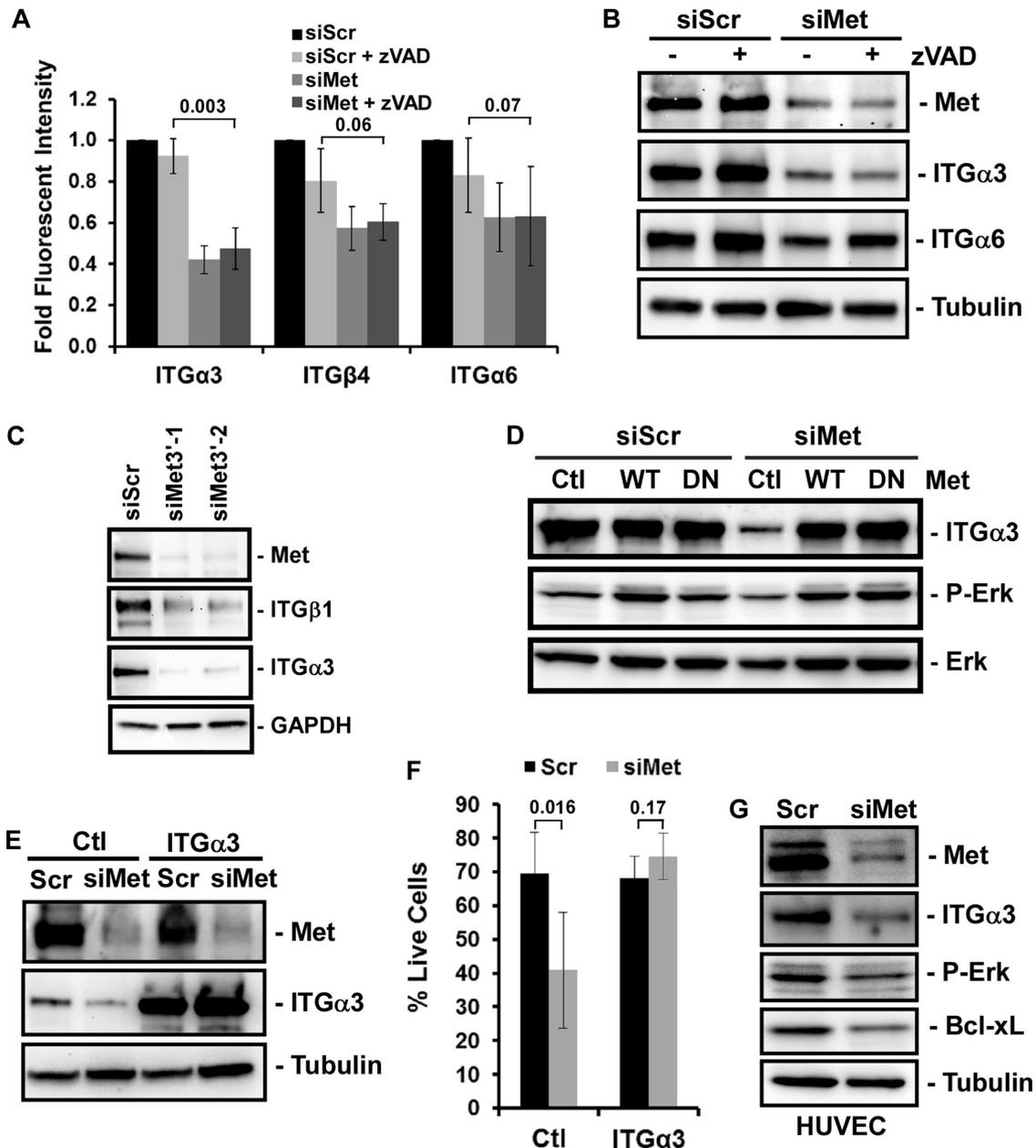
FIGURE 6: Met is required to maintain integrin α3β1 expression. PrECs transfected with scrambled (siScr) or Met (siMet) siRNA in starvation medium and plated on endogenous laminin. (A) Surface levels of integrin α3 (ITGα3), integrin β4 (ITGβ4), and integrin α6 (ITGα6) measured by FACS 24 h after transfection and treatment with vehicle or 20 μM zVAD. The fold increase in fluorescence intensity is relative to cells treated with scrambled siRNA. Error bars are SD; $n = 4$. (B) Met, integrin α3 (ITGα3), integrin α6 (ITGα6), and tubulin measured by immunoblotting 72 h after transfection and treatment with vehicle (−) or 20 μM zVAD (+). (C) Met, integrin β1 (ITGβ1), integrin α3 (ITGα3), and GAPDH assessed by immunoblotting. (D–F) PrECs infected with empty adenovirus vector (Ctl) or virus expressing human siRNA-resistant WT or DN Met or human integrin α3 (ITGα3) 16 h before siRNA transfection. (D) Integrin α3 (ITGα3), activated Erk (P-Erk), and total Erk assessed by immunoblotting. (E) Met, integrin α3 (ITGα3), and tubulin assessed by immunoblotting. (F) Cell viability assessed by trypan blue exclusion. Error bars are SD; $n = 5$; p values are as indicated. (G) HUVEC cells starved and transfected with scrambled (siScr) or Met (siMet) siRNA. Met, integrin α3 (ITGα3), activated Erk (P-Erk), Bcl-xL, and tubulin were measured by immunoblotting.

highlights the importance of defining the involvement of specific steps to fully determining how adhesion affects autophagy.

In summary, the receptor tyrosine kinase Met plays a functional role in contributing to cell survival through maintenance of integrin α3β1. This is mediated independently of Met kinase activity but depends on the Met extracellular and transmembrane domains. Integrin α3β1 is required for matrix-adherent cells to survive starvation by

activating autophagy and escape death due to activation of intrinsic and extrinsic apoptosis pathways.

MATERIALS AND METHODS
Cell culture
Primary cultures of human PrECs derived from normal human prostatic tissues were isolated and cultured as previously described
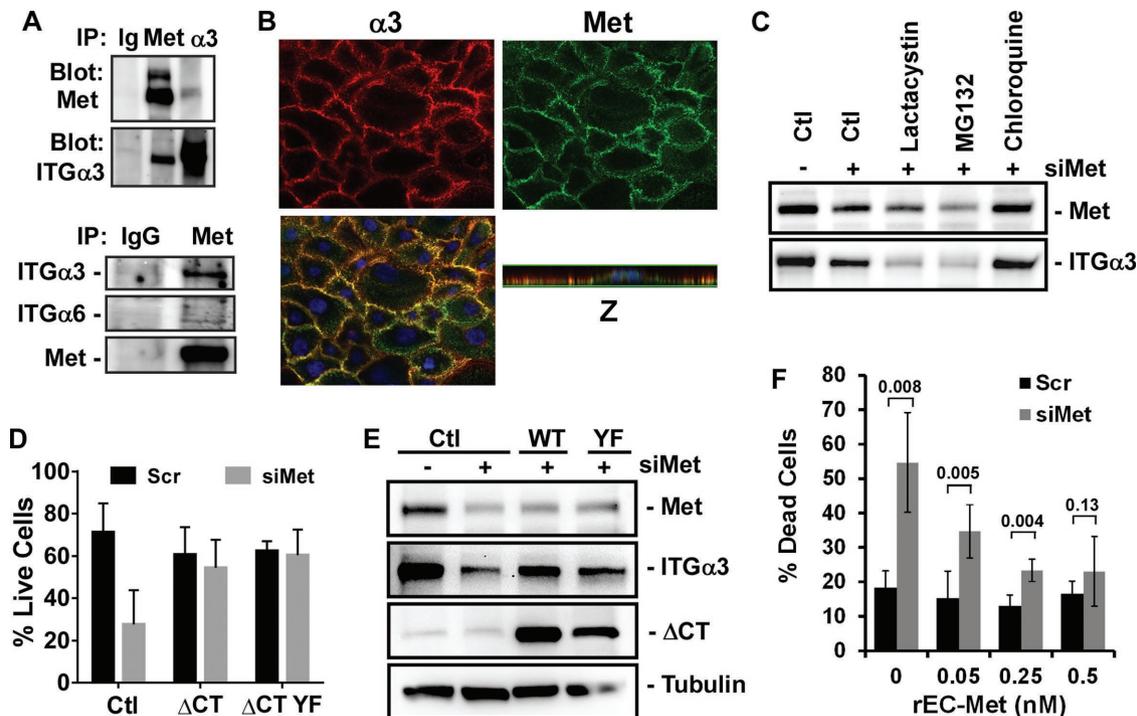
FIGURE 7: Met extracellular domain is required for survival. (A) Integrin α3 or Met immunoprecipitated from laminin-adherent PrECs and their association with Met, integrin α3, and integrin α6 assessed by immunoblotting. (B) Localization of Met (green) and integrin α3 (red) assessed by immunostaining of PrECs and scanning confocal fluorescence microscopy. Z, compiled z-stack from confocal scan. (C) PrECs transfected with Met (+) or scrambled (−) siRNA (siMet) and adherent to endogenous laminin in the absence (Ctl) or presence of 10 μM lactacystin, 5 μM MG132, or 20 μM chloroquine. Met and integrin α3 expression assessed by immunoblotting. (D, E) PrECs infected with empty adenovirus vector (Ctl) or virus expressing human siRNA-resistant cytoplasmic deletion (ΔCT) Met with WT or a Y1003F (YF) mutation and then transfected with Met (siMet, +) or scrambled (siScram, −) siRNA. (D) Cell viability assessed by trypan blue exclusion. (E) Endogenous Met, integrin α3, ΔCT Met, and tubulin assessed by immunoblotting. (F) PrECs transfected with Met (siMet) or scrambled (siScr) siRNA and adherent to laminin treated with IgG/BSA (0) or increasing concentrations (nM) of recombinant extracellular Fc-Met protein (rEC-Met) in BSA. Cell viability was measured by trypan blue exclusion. Error bars are SD; n = 4; p values are as indicated.

(Gmyrek *et al.*, 2001). PrECs were maintained in Keratinocyte-SFM medium (Invitrogen, Waltham, MA) supplemented with bovine pituitary extract and EGF. All analyses were carried out in cells between passages 3 and 5. Three different human isolates were used in these studies. For all experiments, PrECs adherent to their endogenous laminin-rich matrix were genetically manipulated in complete medium, starved, and then replated in Keratinocyte-SFM medium without supplements to allow readhesion to endogenous matrix. The cells were analyzed 24–72 h later. For the rescue experiments, cells were first infected with adenovirus expressing human siMet-resistant Met or integrin α3 and then transfected 16 h later with siRNA. Cells were assessed 48 h after transfection. Primary cultures of mouse prostate epithelial cells were obtained from the prostates of Met^{fl/fl} or Met^{fl/fl} × Cre-ER[TM] male mice (Hayashi and McMahon, 2002; Chmielowiec *et al.*, 2007). Cells were isolated and cultured in Prosta-Cult medium as described by the manufacturer (Stem Cell Technologies, Vancouver, Canada), except that the isolated cells were placed on plates coated with10 μg/ml rat-tail collagen (BD Biosciences). HUVEC cells were obtained from the American Type Culture Collection (ATCC; Manassas, VA) and cultured as recommended.

Antibodies
Immunoblotting. Polyclonal Met (C-28) antibody was purchased from Santa Cruz Biotechnology (Dallas, TX) (cytoplasmic domain) and monoclonal Met (4F8.2) from Millipore (Ontario, Canada)

(extracellular domain). Anti–α-tubulin was purchased from Sigma-Aldrich (St. Louis, MO), caspase 3, Bcl-xL, LC3, LAMP2, and phospho-Erk1/2 (T202/Y204) antibodies were purchased from Cell Signaling (Danvers, MA). The anti-phosphotyrosine monoclonal antibody 4G10 was obtained from Millipore. EGFR (Ab12) monoclonal antibody was purchased from NeoMarkers (Fremont, CA). Monoclonal Erk1/2 antibodies were purchased from Becton-Dickinson Transduction Labs (Franklin Lakes, NJ). Polyclonal goat mouse-specific anti-Met antibody (AF527) was from R&D Systems (Minneapolis, MN). Integrin α6 polyclonal antibody was provided by Anne Cress (University of Arizona, Phoenix, AZ; Pawar *et al.*, 2007). Integrin α3 immunoblotting polyclonal antibody was provided by Chris Stipp (University of Iowa, Iowa City, IA).

Immunoprecipitation. EGFR monoclonal antibodies were purified from hybridoma HB-8508 obtained from the ATCC. Met immunoprecipitating monoclonal antibody, D1, was provided by the Van Andel Institute Antibody Core. Immunoprecipitating α3 monoclonal antibody, A3-X8, was provided by Chris Stipp (Winterwood *et al.*, 2006).

Fluorescence-activated cell sorting, blocking, and immunostaining
Monoclonal α3 clone ASC-1 and β4 integrin clone ASC-3 were purchased from Chemicon (Ontario, Canada), and rat polyclonal α6
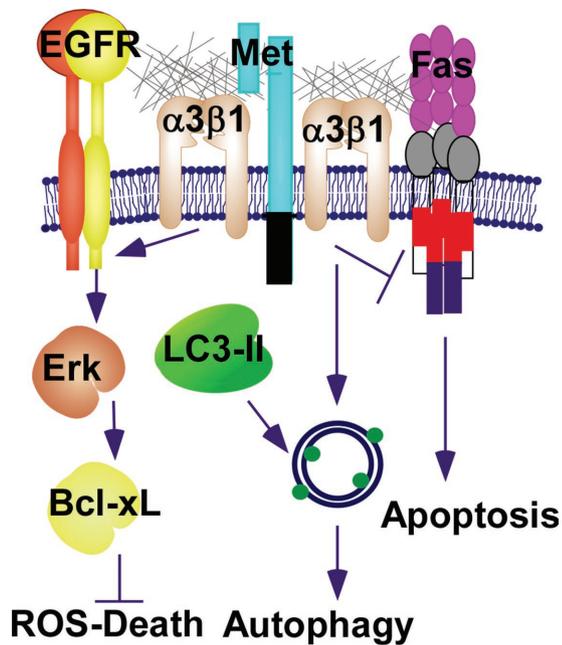
FIGURE 8: Model for Met and integrin α3–mediated survival. The extracellular and transmembrane domain of Met (cyan), but not the cytoplasmic tail (black), is required for cell survival on matrix via regulation of a potential complex with integrin α3β1 and Fas. Met-mediated maintenance of integrin α3β1 is required to suppress ROS-mediated death through induction of EGFR/Erk signaling, inhibit apoptosis by suppressing Fas, and promote autophagy-mediated survival under growth factor starvation conditions.

clone GoH3 was purchased from BD PharMingen (San Jose, CA). Polyclonal antibody to human Met was from R&D (AF276), and the immunostaining integrin α3 (P1F2-1-1) antibody was a gift from William Carter (Fred Hutchinson Cancer Research Center, Seattle, WA; Symington and Carter, 1995). Fas receptor blocking antibody ZB4 was purchased from Millipore. Anti–annexin V conjugated to Alexa Fluor 568 came from Molecular Probes. Horseradish peroxidase–conjugated secondary antibodies for immunoblotting, rabbit anti-mouse and goat anti-rabbit, were purchased from Santa Cruz Biotechnology. Alexa Fluor 488 and 563 goat anti-rat, mouse anti-rabbit, and rabbit anti-mouse were purchased from Molecular Probes. Control immunoglobulin Gs (IgGs; rat, mouse, rabbit) were purchased from Pierce.

Molecular constructs

Full-length human Met cDNA in pMOG was provided by George Vande Woude (Van Andel Institute, Grand Rapids, MI). The SalI and NdeI Met restriction fragment of the extracellular domain was subcloned into pET-DuetI and used to generate the siMet-resistant WT Met by site-directed mutagenesis of three base pairs within the si-Met target sequence (siMet1251) targeted to the extracellular domain using the Stratagene Mutagenesis Kit. The primer sequence was 5′-AGATTCTGCCGAACCAATGGACCGGTCCGCCATGTGTG CATTCCC-3′. The full mutagenized fragment was sequenced to verify fidelity. The Met SalI and NdeI fragment was then subcloned back into full-length pMOG Met, and then full-length Met was subcloned into pShuttle-CMV (Stratagene) via XhoI and HindIII to generate pShuttle-CMV/mut3huMet.

KD siMet-resistant Met cDNA was generated by cutting out the 1.4-kb SpeI/HindIII fragment of pMOG/huMet and subcloned into BlueScript to generate KD Met K1110M (Furge et al., 2001) by site-directed mutagenesis using the Stratagene Mutagenesis Kit. The

primer sequence was 5′-AAATTCACTGTGCTGTGATGTCCTT-GAACAGAATCACTGA-3′. The SpeI/HindIII mutated fragment was then subcloned into pShuttle-CMV/mut3huMet to generate pShuttle-CMV/DNmut3huMet. Human pMB23-Tpr-Met was provided by George Vande Woude (Gonzatti-Haces et al., 1988). Tpr-Met was subcloned into pcDNA3.1 using EcoRI. Tpr-Met was subsequently subcloned into pShuttle-CMV via KpnI and XhoI to generate pShuttle-CMV/Tpr-Met. To generate the cytoplasmic truncation mutant ΔCT, mut3huMet (siRNA-resistant) was PCR cloned to include amino acids Met1–Arg1022 and ligated into pENTR3C at KpnI and XhoI. PCR cloning primer sequences were as follows: forward, 5′-AATGGTACCCACCGAAAGATAAACCTCTC; and reverse, 5′-AAACTCGAGTGTCGGCATGAACCGTTC. After sequence verification, it was recombined into pAD-CMV-V5-DEST. Mutagenesis of Y1003 to F1003 (YF) of pENTR3C-ΔCT-Met was done using the QuikChange Site-Directed Mutagenesis Kit (Stratagene, La Jolla, CA) and primer 5′-GAATCTGTAGACTTCCGAGCTACTTTTCC-3′. The sequence-verified clone was recombined into pAD-CMV-V5-DEST. Human integrin (ITG) α3 was PCR cloned out of pZeo-ITGα3 (a gift of M. DiPersio, Albany Medical College, Albany, NY) and ligated into KpnI and NotI sites of Gateway pENTR3C (Life Technologies, Waltham, MA). Then pENTR3C-ITGα3 was recombined into Gateway pAd-CMV-V5-DEST (Life Technologies). PCR primer sequences were as follows: forward, 5′-TATGGTACCACGCGCTCTC-GCC-3′; and reverse, 5′-AAAGCGGCCGCAAAGAAGTCACACC-3′. Met shRNA U6-pShuttle-GFP was generated by subcloning hybridized DNA oligomers containing specific shRNA sequences with SalI and BglII restriction sites. shRNA oligo sequences were as follows: shRNA1, 5′-TCGACCAATGGATCGATCTGCCAGAGTACTGTGGC-AGATCGATCCATTGGTT TTTT-3′; shRNA2, 5′-TCGATGTGTCGC-TCCGTATCCTTGAGTACTGAAGGATACGGAGCGACA-CATTTTTT-3′; and scrambled sequence, 5′-TCGAACTACCGTTGT-TATAGGTGGAGTACTGCACCTATAACAACGGTAGTTTTTTT-3′. pShuttle constructs containing LC3-GFP (Edick et al., 2007), GFP-Cre (courtesy of George Vande Woude), Met, or shRNAs were used to generate pAd-Easy (Stratagene) adenoviral recombinants in BJ5183-AD1 bacteria.

Adenovirus

HEK293 cells were transfected with 5 µg of linearized adenoviral recombinant DNA constructs using Lipofectamine 2000. As soon as cytopathic effects appeared at 3–5 d, cells were harvested and lysed by freeze-thawing and adenoviruses purified and titered in PrECs using a kit from Clontech. PrECs were routinely infected at a multiplicity of infection (MOI) of 1–2 for cDNAs and 2–5 for shRNAs. For viral constructs independently expressing GFP, immunofluorescence imaging indicated that the MOI was sufficient to generate an infection rate of >95%. Immunoblotting verified that the MOI was sufficient to knock down Met expression by 85–90%.

siRNA

Several Met-specific siRNAs—siMet1251 (human specific), siMet4268 (cross species), and two 3′ untranslated region (siMet3′-1,2)—as well as a scrambled siRNA, were ordered from Integrated DNA Technologies (Coralville, IA) and annealed to generate double-stranded siRNAs. An additional Met-targeted siRNA, siMet565, was tested, but it failed to block Met expression and was used as a second control siRNA (shMetMut). siRNA sequences were as follows: siMet1251, 5′-AACCAATGGATCGATCTGCCA-3′; siMet4268, 5′-AATGTGT-CGCTCCGTATCCTT-3′; siMet565 (shMetMut), 5′-AAGGACCG-GTTCATCAACTTC-3′; siMet3′-1, 5′-CTACCAGGGTTCAAGAGCAT-GAACGC-3′, siMet3′-2, 5′- CACCCATTAGGTAAACATTCCCUTT-3′;

and scrambled, 5'-ACTACCGTTGTTATAGGTG-3'. siRNAs between 5 and 30 nM were introduced into PrECs using SiLentfect lipid from Bio-Rad (Hercules, CA), and the lowest concentration of siRNA giving the most effective knockdown was subsequently used. Control studies using fluorescently labeled control siRNAs indicated >90% transfection efficiency in PrECs.

Inhibitors

PrECs adherent to endogenous laminin matrix and starved for 24 h were treated with 1 µM staurosporine (Promega, Madison, WI), 10–20 µM SU11274 (Calbiochem, Ontario, Canada), or 0.1–1 µM PHA665752 (provided by James Christensen, Pfizer, La Jolla, CA). Cells were incubated for 24–72 h. The working concentration of the Met pharmacological inhibitors was determined by titrating to the minimum inhibitor concentration that effectively blocked tyrosine phosphorylation of Met for 72 h. Caspase 3/7 inhibitor, zVAD-FMK, was purchased from Promega and caspase 8 inhibitor, zIETD-fmk, from Sigma-Aldrich. Both were used at 20 µM and added 16 h after siRNA transfection. Lactacystin, MG132, and chloroquine were purchased from Sigma-Aldrich.

Peptide rescue

Human recombinant Met, consisting of the cleaved and cytseine-bonded α- and β-chains of the Met extracellular domain fused to Fc (rEC-Met), was purchased from R&D Systems and reconstituted in bovine serum albumin (BSA) as directed. At 16 h after siRNA Met transfection, cells were treated with IgG/BSA or concentrations of peptide from 0.01 to 0.1 nM.

Met$^{fl/fl}$ mice

Met$^{fl/+}$ mice (Chmielowiec et al., 2007) and Cre-ER^{TM} mice (Hayashi and McMahon, 2002) were obtained from the Van Andel Research Institute Mouse Repository and bred to generate Met$^{fl/fl}$ or Cre-ER^{TM}/Met$^{fl/fl}$ mice. Prostate epithelial cells were isolated from 6- to 10-wk-old adult male mice as described. After 1 d in culture, cells were either infected with Cre adenovirus (Met$^{fl/fl}$) or treated with 1.5 µM tamoxifen (Cre-ER^{TM}/Met$^{fl/fl}$) to induce loss of Met expression. Cell viability and biochemical analyses were conducted 24 h later. Institutional Animal Care and Use Committee protocol approval was obtained for these studies in compliance with all relevant federal guidelines and institutional policies.

Cell viability assays

Trypan blue exclusion. Cell viability was measured 48–72 h posttransfection with siRNAs. Cells were trypsinized and counted after exposure to trypan blue. Cells not taking up the dye were considered to be viable.

ATP levels. Cell viability was assayed using the CellTiter-Glo Luminescent Assay kit (Promega) following the manufacturer's protocol. This assay determines cell viability based on quantification of intracellular ATP levels. Approximately 10,000 cells/well were allowed to adhere to endogenous laminin matrix in BSA-coated 96-well plates. CellTiter-Glo reagent was added 24–72 h after inhibitor or siRNA or shRNA treatment and incubated for 1 h at room temperature in the dark. Relative light intensity was measured in each well using a Fluoroskan Assent FL fluorometer and software (Labsystems).

Annexin V

Annexin V was measured using a kit obtained from Molecular Probes (Invitrogen). Cells were resuspended in annexin binding buffer (10 mM 4-(2-hydroxyethyl)-1-piperazineethanesulfonic acid, 140 mM NaCl, 2.5 mM CaCl$_2$, pH 7.4) containing Alexa Fluor 568–conjugated annexin V and incubated in the dark for 15 min. Samples were put on ice and immediately analyzed. The extent of staining was monitored by fluorescence-activated cell sorting (FACS) using a FACSCalibur (Becton-Dickinson) and CellQuest acquisition and analysis software (Becton-Dickinson) immediately after staining. On several occasions, annexin V staining was also monitored in adherent cells using a Nikon Eclipse TE300 fluorescence microscope and quantified using OpenLab image analysis software (ImProVision).

Caspase activity

The CaspaseGlo 3/7 kit (Promega) was used to measure caspase 3 and 7 activities following the manufacturer's protocol. Approximately 10,000 cells/well were allowed to adhere to endogenous laminin in BSA-coated 96-well plates. CaspaseGlo reagent was added 24–72 h after inhibitor or siRNA or shRNA treatment and incubated for 1 h at room temperature in the dark. Relative light intensity was measured in each well using a Fluoroskan Assent FL fluorometer and software (Labsystems, Waltham, MA). In addition, total caspase 3 levels were monitored by immunoblotting, with decreased levels of caspase 3 being associated with increased cell death.

Immunoprecipitation and immunoblotting

For protein analyses of whole-cell lysates, cells were lysed in RIPA (10 mM Tris, pH 7.2, 158 mM NaCl, 1 mM EDTA, 0.1% SDS, 1% NaDOC, 1% Triton X-100, 1 mM Na$_3$VO$_4$, 1 mM phenylmethylsulfonyl fluoride [PMSF], 100 U/ml aprotinin, 10 µg/ml pepstatin, and 10 µg/ml leupeptin) and protein concentrations determined by bicinchoninic acid assay (Pierce). For coimmunoprecipitation studies, cells were lysed in Triton X-100 buffer (50 mM Tris, pH 7.5, 100 mM NaCl, 0.5 mM EDTA, 1% Triton X-100, 50 mM NaF, 50 mM β-glycerophosphate, 5 mM sodium pyrophosphate, 1 mM Na$_3$VO$_4$, 1 mM PMSF, 100 U/ml aprotinin, 10 µg/ml pepstatin, and 10 µg/ml leupeptin). Immunoprecipitation and immunoblotting conditions were carried out as previously described (Edick et al., 2007). Chemiluminescence signal was captured by a charge-coupled device (CCD) camera in a Bio-Rad Chemi-Doc Imaging System. Where necessary, blots were stripped and reprobed for total levels of protein in the immunoprecipitates or cell lysates.

Autophagy assays

LC3-GFP. PrECs were infected at MOI of 1–2 with adenoviruses expressing LC3-GFP (Edick et al., 2007). Twenty-four hours later, cells were growth factor–deprived and transfected with Met or scrambled siRNA. Localization of GFP-LC3 was monitored by a standard fluorescence microscopy at 24 and 48 h posttransfection using a Nikon Eclipse TE300 fluorescence microscope and OpenLab image analysis software (ImProVision, Waltham, MA). For quantification, cells displaying at least 10 punctate spots were scored as positive for LC3II staining.

LC3 Immunoblotting. Expression of endogenous LC3 was measured by immunoblotting. PrECs were transfected with Met or scrambled siRNA, starved, and plated on endogenous laminin for 48 h and then treated with dimethyl sulfoxide (DMSO) or 4 µM chloroquine several hours before lysis to inhibit lysosomal function. Levels of LC3-I and LC3-II and LAMP2 were monitored by immunoblotting.

FACS

Cell surface expression of α3β1 or α6β4 integrin was measured by FACS. Cells were treated with dissociation buffer and then lightly

trypsinized. Cells were stained with corresponding primary antibody anti-ITGα3, ITGβ4, or ITGα6 for 1 h at 4°C. After several washes, Alexa Fluor–labeled secondary antibodies were applied and incubated for 1 h at 4°C. Samples were put on ice and immediately analyzed. The extent of staining was monitored using a FACSCalibur and CellQuest acquisition and analysis software.

Immunofluorescence staining
Starved PrECs were placed in eight-chamber slides (LabTek) at a density of 1×10^4 cells/chamber and allowed to adhere to endogenous LM5 matrix for 72 h. Cells were fixed with 4% formaldehyde for 20 min at room temperature. Slides were washed three times with Dulbecco's phosphate-buffered saline (PBS) and then washed times with 100 mM glycine in PBS for 5–10 min per wash. Slides were blocked with 5% BSA in PBS for 2 h at room temperature. Slides were first incubated for 20 h at 4°C with goat anti-Met AF527 antibody (R&D Systems) diluted 1:75 in 5% BSA/PBS and then washed. All washes were done three times for 5–10 min per wash using PBS containing 0.1% BSA and 0.05% Tween 20. Slides were further incubated with mouse anti-ITGα3 antibody (PIF2) diluted 1:10 in 5% BSA/PBS for 20 h and then washed. Mouse secondary Alexa Fluor 546 and goat secondary Alexa Fluor 488 (Invitrogen), each diluted 1:500 in 5% BSA/PBS, were added for 1 h at room temperature, and then slides were again washed. Nuclei were stained with Hoechst 33258 (Sigma-Aldrich) at 1.25 µg/ml in 5% BSA/PBS for 10 min at room temperature. Finally, slides were washed three times in BSA/Tween 20/PBS and then three times with water and then mounted with aqueous gel mounting medium (Biomedia, St. Louis, MO). Images were acquired either by epifluorescence with a Nikon Eclipse TE300 microscope and Hamamatsu CCD video camera using OpenLab Imaging software (ImproVision) or by confocal microscopy using sequential detection on an Olympus FluoView 1000 LSM using FluoView software, version 5.0.

REFERENCES
Aoudjit F, Vuori K (2001). Matrix attachment regulates Fas-induced apoptosis in endothelial cells: a role for c-flip and implications for anoikis. J Cell Biol 152, 633–643.

Berditchevski F, Gilbert E, Griffiths MR, Fitter S, Ashman L, Jenner SJ (2001). Analysis of the CD151-alpha3beta1 integrin and CD151-tetraspanin interactions by mutagenesis. J Biol Chem 276, 41165–41174.

Bill HM, Knudsen B, Moores SL, Muthuswamy SK, Rao VR, Brugge JS, Miranti CK (2004). Epidermal growth factor receptor-dependent regulation of integrin-mediated signaling and cell cycle entry in epithelial cells. Mol Cell Biol 24, 8586–8599.

Boisvert-Adamo K, Aplin AE (2008). Mutant B-RAF mediates resistance to anoikis via Bad and Bim. Oncogene 27, 3301–3312.

Boisvert-Adamo K, Longmate W, Abel EV, Aplin AE (2009). Mcl-1 is required for melanoma cell resistance to anoikis. Mol Cancer Res 7, 549–556.

Chmielowiec J, Borowiak M, Morkel M, Stradal T, Munz B, Werner S, Wehland J, Birchmeier C, Birchmeier W (2007). c-Met is essential for wound healing in the skin. J Cell Biol 177, 151–162.

Christensen JG, Schreck R, Burrows J, Kuruganti P, Chan E, Le P, Chen J, Wang X, Ruslim L, Blake R, et al. (2003). A selective small molecule inhibitor of c-Met kinase inhibits c-Met-dependent phenotypes in vitro and exhibits cytoreductive antitumor activity in vivo. Cancer Res 63, 7345–7355.

Coll ML, Rosen K, Ladeda V, Filmus J (2002). Increased Bcl-xL expression mediates v-Src-induced resistance to anoikis in intestinal epithelial cells. Oncogene 21, 2908–2913.

Cowin AJ, Adams D, Geary SM, Wright MD, Jones JC, Ashman LK (2006). Wound healing is defective in mice lacking tetraspanin CD151. J Invest Dermatol 126, 680–689.

Edick MJ, Tesfay L, Lamb LE, Knudsen BS, Miranti CK (2007). Inhibition of integrin-mediated crosstalk with epidermal growth factor receptor/Erk or Src signaling pathways in autophagic prostate epithelial cells induces caspase-independent death. Mol Biol Cell 18, 2481–2490.

Flusberg DA, Numaguchi Y, Ingber DE (2001). Cooperative control of Akt phosphorylation, bcl-2 expression, and apoptosis by cytoskeletal microfilaments and microtubules in capillary endothelial cells. Mol Biol Cell 12, 3087–3094.

Frisch SM (1999). Evidence for a function of death-receptor-related, death-domain-containing proteins in anoikis. Curr Biol 9, 1047–1049.

Frisch SM, Screaton RA (2001). Anoikis mechanisms. Curr Opin Cell Biol 13, 555–562.

Frisch SM, Vuori K, Kelaita D, Sicks S (1996). A role for Jun-N-terminal kinase in anoikis; suppression by bcl-2 and crmA. J Cell Biol 135, 1377–1382.

Furge KA, Kiewlich D, Le P, Vo MN, Faure M, Howlett AR, Lipson KE, Woude GF, Webb CP (2001). Suppression of Ras-mediated tumorigenicity and metastasis through inhibition of the Met receptor tyrosine kinase. Proc Natl Acad Sci USA 98, 10722–10727.

Gan L, Liu P, Lu H, Chen S, Yang J, McCarthy JB, Knudsen KE, Huang H (2009). Cyclin D1 promotes anchorage-independent cell survival by inhibiting FOXO-mediated anoikis. Cell Death Differ 16, 1408–1417.

Garcia-Martinez JM, Calcabrini A, Gonzalez L, Martin-Forero E, Agullo-Ortuno MT, Simon V, Watkin H, Anderson SM, Roche S, Martin-Perez J (2010). A non-catalytic function of the Src family tyrosine kinases controls prolactin-induced Jak2 signaling. Cell Signal 22, 415–426.

Gilmore AP (2005). Anoikis. Cell Death Differ 12, 1473–1477.

Gmyrek GA, Walburg M, Webb CP, Yu HM, You X, Vaughan ED, Vande Woude GF, Knudsen BS (2001). Normal and malignant prostate epithelial cells differ in their response to hepatocyte growth factor/scatter factor. Am J Pathol 159, 579–590.

Gomez-Quiroz LE, Factor VM, Kaposi-Novak P, Coulouarn C, Conner EA, Thorgeirsson SS (2008). Hepatocyte-specific c-Met deletion disrupts redox homeostasis and sensitizes to Fas-mediated apoptosis. J Biol Chem 283, 14581–14589.

Gonzatti-Haces M, Seth A, Park M, Copeland T, Oroszlan S, Vande Woude GF (1988). Characterization of the TPR-MET oncogene p65 and the MET protooncogene p140 protein-tyrosine kinases. Proc Natl Acad Sci USA 85, 21–25.

Grunwald IC, Korte M, Wolfer D, Wilkinson GA, Unsicker K, Lipp HP, Bonhoeffer T, Klein R (2001). Kinase-independent requirement of EphB2 receptors in hippocampal synaptic plasticity. Neuron 32, 1027–1040.

Harnois C, Demers MJ, Bouchard V, Vallee K, Gagne D, Fujita N, Tsuruo T, Vezina A, Beaulieu JF, Cote A, et al. (2004). Human intestinal epithelial crypt cell survival and death: Complex modulations of Bcl-2 homologs by Fak, PI3-K/Akt-1, MEK/Erk, and p38 signaling. J Cell Physiol 198, 209–222.

Hayashi S, McMahon AP (2002). Efficient recombination in diverse tissues by a tamoxifen-inducible form of Cre: a tool for temporally regulated gene activation/inactivation in the mouse. Dev Biol 244, 305–318.

Higuchi M, Onishi K, Kikuchi C, Gotoh Y (2008). Scaffolding function of PAK in the PDK1-Akt pathway. Nat Cell Biol 10, 1356–1364.

Huh CG, Factor VM, Sanchez A, Uchida K, Conner EA, Thorgeirsson SS (2004). Hepatocyte growth factor/c-met signaling pathway is required

for efficient liver regeneration and repair. Proc Natl Acad Sci USA 101, 4477–4482.

Humbert M, Medova M, Aebersold DM, Blaukat A, Bladt F, Fey MF, Zimmer Y, Tschan MP (2013). Protective autophagy is involved in resistance towards MET inhibitors in human gastric adenocarcinoma cells. Biochem Biophys Res Commun 431, 264–269.

Ishibe S, Karihaloo A, Ma H, Zhang J, Marlier A, Mitobe M, Togawa A, Schmitt R, Czyczk J, Kashgarian M, et al. (2009). Met and the epidermal growth factor receptor act cooperatively to regulate final nephron number and maintain collecting duct morphology. Development 136, 337–345.

Klosek SK, Nakashiro K-i, Hara S, Goda H, Hasegawa H, Hamakawa H (2009). CD151 regulates HGF-stimulated morphogenesis of human breast cancer cells. Biochem Biophys Res Commun 379, 1097–1100.

Knudsen BS, Vande Woude G (2008). Showering c-MET-dependent cancers with drugs. Curr Opin Genet Dev 18, 87–96.

Kreidberg JA, Donovan MJ, Goldstein SL, Rennke H, Shepherd K, Jones RC, Jaenisch R (1996). Alpha 3 beta 1 integrin has a crucial role in kidney and lung organogenesis. Development 122, 3537–3547.

Luo M, Zhao X, Chen S, Liu S, Wicha MS, Guan JL (2013). Distinct FAK activities determine progenitor and mammary stem cell characteristics. Cancer Res 73, 5591–5602.

Manohar A, Shome SG, Lamar J, Stirling L, Iyer V, Pumiglia K, DiPersio CM (2004). a3b1 integrin promotes keratinocyte cell survival through activation of a MEK/ERK signaling pathway. J Cell Sci 117, 4043–4054.

Marconi A, Atzei P, Panza C, Fila C, Tiberio R, Truzzi F, Wachter T, Leverkus M, Pincelli C (2004). FLICE/caspase-8 activation triggers anoikis induced by beta1-integrin blockade in human keratinocytes. J Cell Sci 117, 5815–5823.

Owens TW, Valentijn AJ, Upton JP, Keeble J, Zhang L, Lindsay J, Zouq NK, Gilmore AP (2009). Apoptosis commitment and activation of mitochondrial Bax during anoikis is regulated by p38MAPK. Cell Death Differ 16, 1551–1562.

Pawar SC, Demetriou MC, Nagle RB, Bowden GT, Cress AE (2007). Integrin alpha6 cleavage: a novel modification to modulate cell migration. Exp Cell Res 313, 1080–1089.

Pomerleau V, Landry M, Bernier J, Vachon PH, Saucier C (2014). Met receptor-induced Grb2 or Shc signals both promote transformation of intestinal epithelial cells, albeit they are required for distinct oncogenic functions. BMC Cancer 14, 240.

Puthalakath H, Villunger A, O'Reilly LA, Beaumont JG, Coultas L, Cheney RE, Huang DC, Strasser A (2001). Bmf: a proapoptotic BH3-only protein regulated by interaction with the myosin V actin motor complex, activated by anoikis. Science 293, 1829–1832.

Reginato MJ, Mills KR, Paulus JK, Lynch DK, Sgroi DC, Debnath J, Muthuswamy SK, Brugge JS (2003). Integrins and EGFR coordinately regulate the pro-apoptotic protein Bim to prevent anoikis. Nat Cell Biol 5, 733–740.

Rosen K, Shi W, Calabretta B, Filmus J (2002). Cell detachment triggers p38 mitogen-activated protein kinase-dependent overexpression of Fas ligand. A novel mechanism of Anoikis of intestinal epithelial cells. J Biol Chem 277, 46123–46130.

Rytomaa M, Martins LM, Downward J (1999). Involvement of FADD and caspase-8 signalling in detachment-induced apoptosis. Curr Biol 9, 1043–1046.

Saftig P, Beertsen W, Eskelinen EL (2008). LAMP-2: a control step for phagosome and autophagosome maturation. Autophagy 4, 510–512.

Schmelzle T, Mailleux AA, Overholtzer M, Carroll JS, Solimini NL, Lightcap ES, Veiby OP, Brugge JS (2007). Functional role and oncogene-regulated expression of the BH3-only factor Bmf in mammary epithelial anoikis and morphogenesis. Proc Natl Acad Sci USA 104, 3787–3792.

Shinomiya N, Gao CF, Xie Q, Gustafson M, Waters DJ, Zhang YW, Vande Woude GF (2004). RNA interference reveals that ligand-independent met activity is required for tumor cell signaling and survival. Cancer Res 64, 7962–7970.

Skurk C, Maatz H, Kim H-S, Yang J, Abid MR, Aird WC, Walsh K (2004). The Akt-regulated forkhead transcription factor FOXO3a controls endothelial cell viability through modulation of the caspase-8 inhibitor FLIP. J Biol Chem 279, 1513–1525.

Sridhar SC, Miranti CK (2006). Tetraspanin KAI1/CD82 suppresses invasion by inhibiting integrin-dependent crosstalk with c-Met receptor and Src kinases. Oncogene 25, 2367–2378.

Symington BE, Carter WG (1995). Modulation of epidermal differentiation by epiligrin and integrin alpha 3 beta 1. J Cell Sci 108, 831–838.

Taddei ML, Giannoni E, Fiaschi T, Chiarugi P (2012). Anoikis: an emerging hallmark in health and diseases. J Pathol 226, 380–393.

Todeschini AR, Dos Santos JN, Handa K, Hakomori SI (2007). Ganglioside GM2-tetraspanin CD82 complex inhibits met and its cross-talk with integrins, providing a basis for control of cell motility through glycosynapse. J Biol Chem 282, 8123–8133.

Valentijn AJ, Gilmore AP (2004). Translocation of full-length Bid to mitochondria during anoikis. J Biol Chem 279, 32848–32857.

Valentijn AJ, Zouq N, Gilmore AP (2004). Anoikis. Biochem Soc Trans 32, 421–425.

Wang X, DeFrances MC, Dai Y, Pediaditakis P, Johnson C, Bell A, Michalopoulos GK, Zarnegar R (2002). A mechanism of cell survival: sequestration of Fas by the HGF receptor Met. Mol Cell 9, 411–421.

Wang R, Ferrell LD, Faouzi S, Maher JJ, Bishop JM (2001). Activation of the Met receptor by cell attachment induces and sustains hepatocellular carcinomas in transgenic mice. J Cell Biol 153, 1023–1034.

Wang R, Kobayashi R, Bishop JM (1996). Cellular adherence elicits ligand-independent activation of the Met cell-surface receptor. Proc Natl Acad Sci USA 93, 8425–8430.

Weihua Z, Tsan R, Huang WC, Wu Q, Chiu CH, Fidler IJ, Hung MC (2008). Survival of cancer cells is maintained by EGFR independent of its kinase activity. Cancer Cell 13, 385–393.

Winterwood NE, Varzavand A, Meland MN, Ashman LK, Stipp CS (2006). A critical role for tetraspanin CD151 in alpha3beta1 and alpha6beta4 integrin-dependent tumor cell functions on laminin-5. Mol Biol Cell 17, 2707–2721.

Yauch RL, Kazarov AR, Desai B, Lee RT, Hemler ME (2000). Direct extracellular contact between integrin alpha(3)beta(1) and TM4SF protein CD151. J Biol Chem 275, 9230–9238.

Zervas CG, Gregory SL, Brown NH (2001). Drosophila integrin-linked kinase is required at sites of integrin adhesion to link the cytoskeleton to the plasma membrane. J Cell Biol 152, 1007–1018.

Zou C, Ma J, Wang X, Guo L, Zhu Z, Stoops J, Eaker AE, Johnson CJ, Strom S, Michalopoulos GK, et al. (2007). Lack of Fas antagonism by Met in human fatty liver disease. Nat Med 13, 1078–1085.